Insights into the linear and non-linear optical characteristics of substituted bi-naphthyl-pyrazolines

Houda El Karout, Chiraz Labassi, Karolina Waszkowska, Nicolas Fournier-Le Ray, Rafik Gatri, Fabienne Gauffre, Arnaud Fihey, Bouchta Sahraoui, Jean-Luc Fillaut

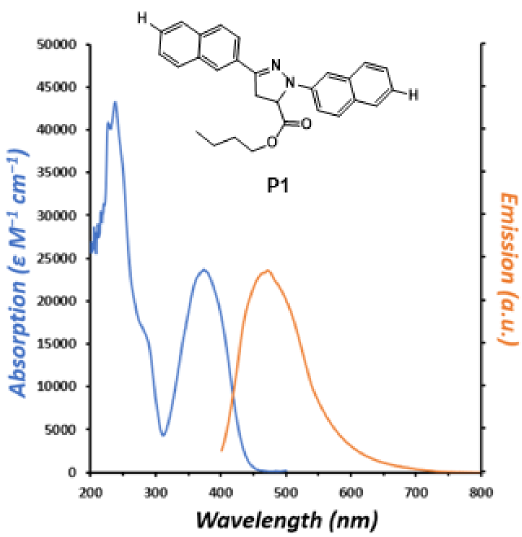

Figure S1: UV–visible absorption and fluorescence emission spectra of pyrazoline **P1** in THF.

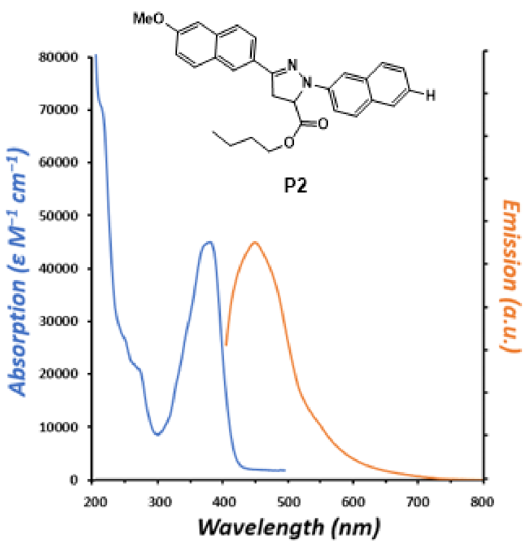

Figure S2: UV–visible absorption and fluorescence emission spectra of pyrazoline **P2** in THF.

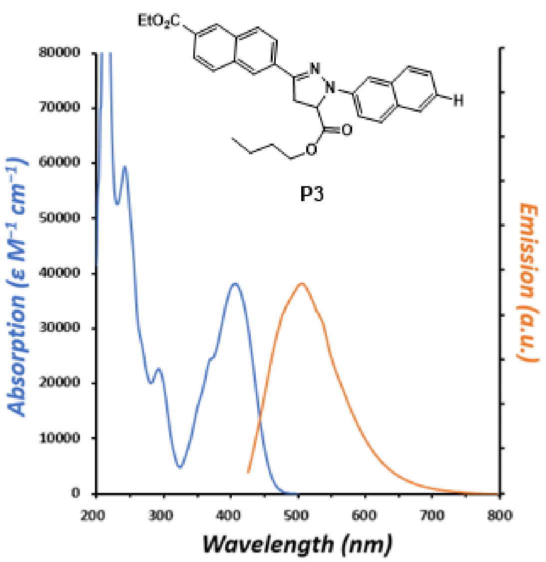

Figure S3: UV–visible absorption and fluorescence emission spectra of pyrazoline **P3** in THF.

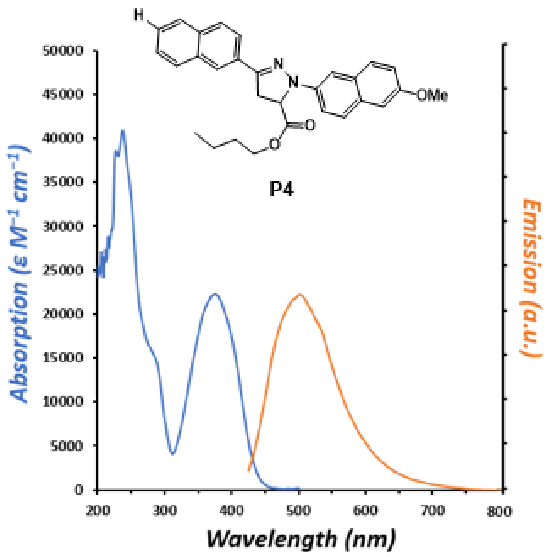

Figure S4: UV–visible absorption and fluorescence emission spectra of pyrazoline **P4** in THF.

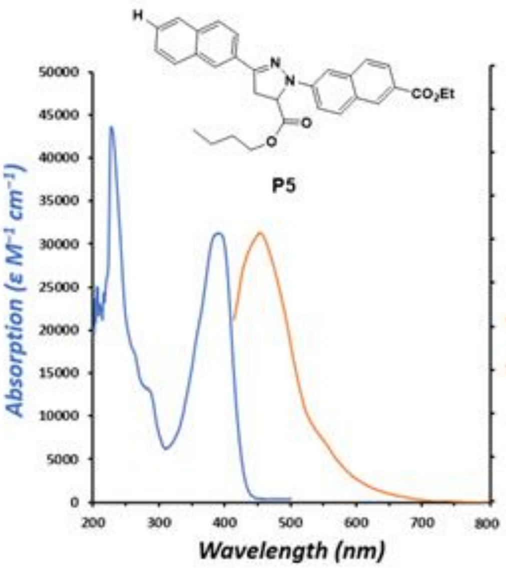

Figure S5: UV–visible absorption and fluorescence emission spectra of pyrazoline **P5** in THF.

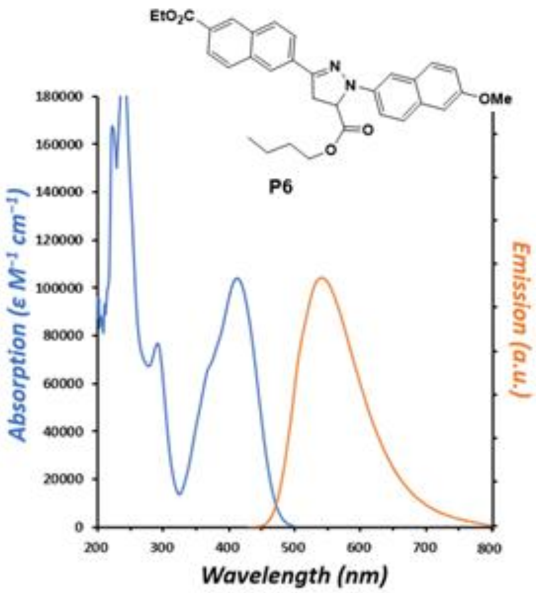

Figure S6: UV–visible absorption and fluorescence emission spectra of pyrazoline **P6** in THF.

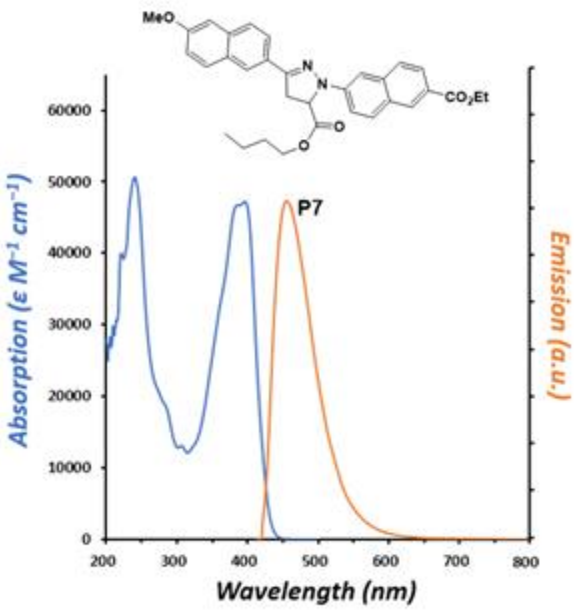

Figure S7: UV–visible absorption and fluorescence emission spectra of pyrazoline **P7** in THF.

THG responses of **P1-7** thin films:

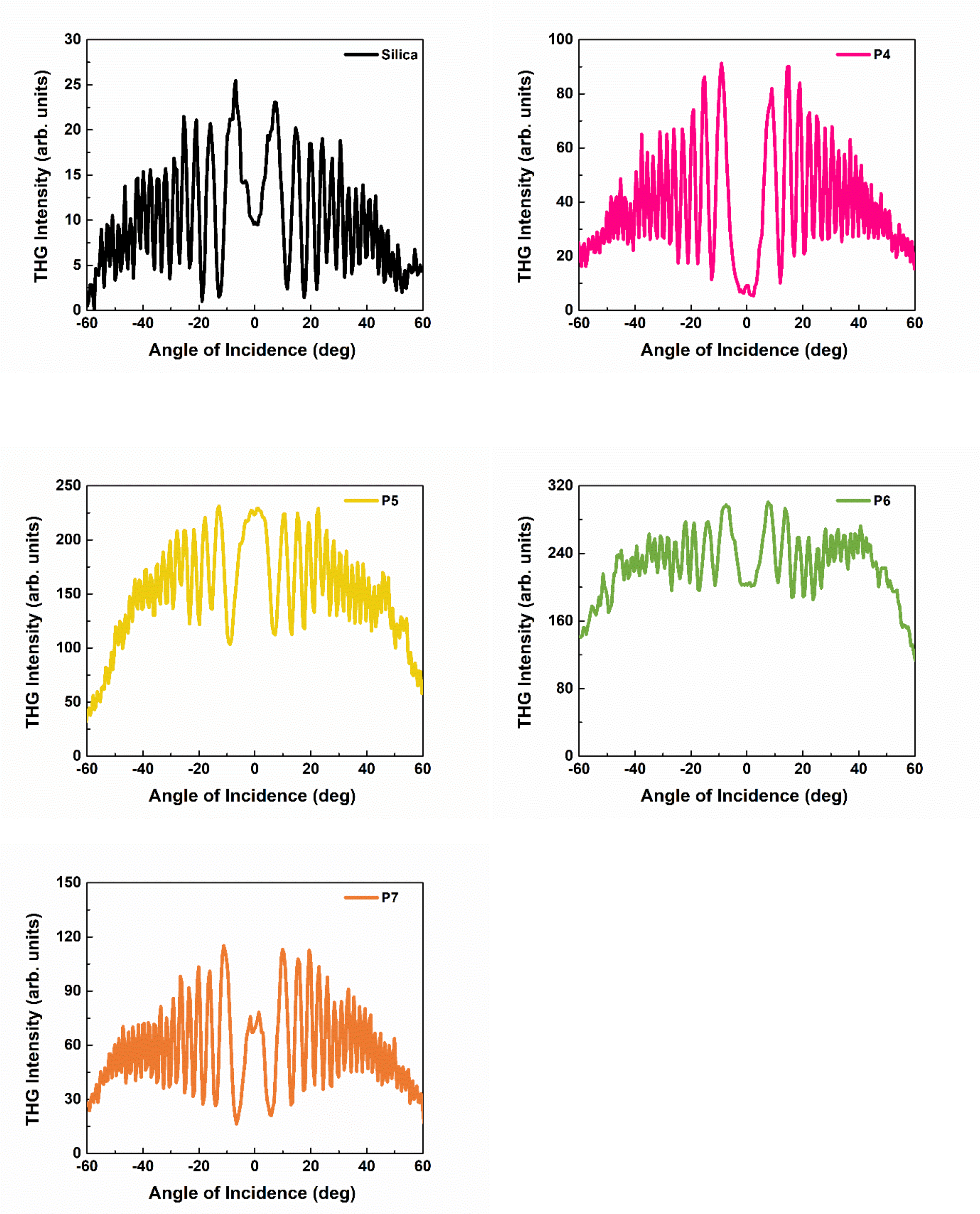

Figure S8: THG intensities as a function of incident angle of investigated thin films in S-P polarized laser irradiation.

Fig. S8 displays THG intensities as a function of incident angle of the studied pyrazoline thin films. Notably, THG process is independent on the laser polarization, therefore it was unnecessary to provide measurements in two configurations.

UV-Vis absorption spectra of P1-7 thin films:

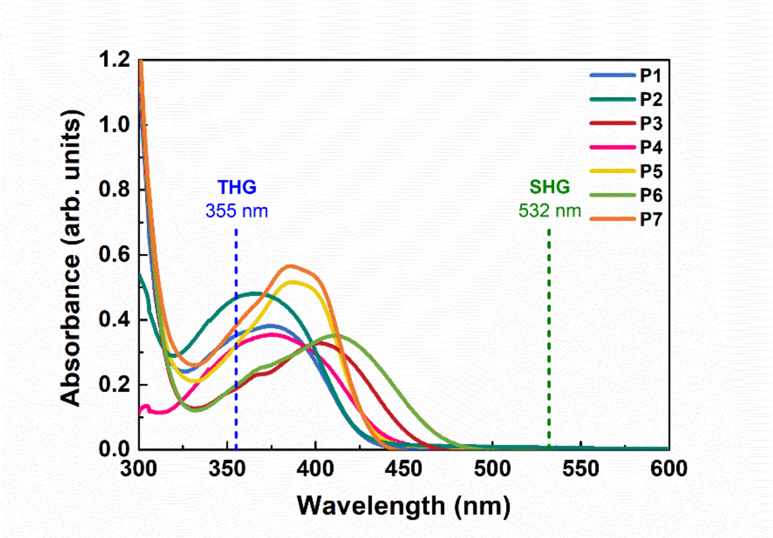

Figure S9: UV-visible absorption spectra of pyrazoline **P1-7** thin films.

Fig. S9 presents UV-visible absorption spectra of investigated pyrazoline **P1-7** thin films. It is important to note that at fundamental laser wavelength, that is 1064 nm, samples are optically transparent. Moreover, at wavelength of 532 nm, which corresponds to generated SH, the absorbance is negligible, however at wavelength corresponding to generated TH, which is 355 nm, absorbance is significant. To clarify, what is generated can be simultaneously be absorbed by the sample. Thus, this consideration was taken in account when calculating 3rd order NLO susceptibility values, using the absorption coefficient in the formula.

$\chi^{(3)}$ values of **P1-7** thin films :

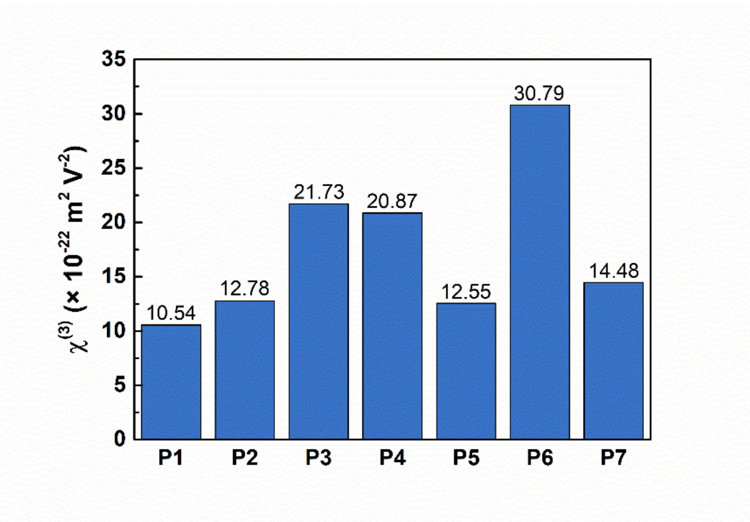

Figure S10: Histogram displaying third-order NLO susceptibilities of **P1-7** thin films.

SHG responses of **P1-7** thin films:

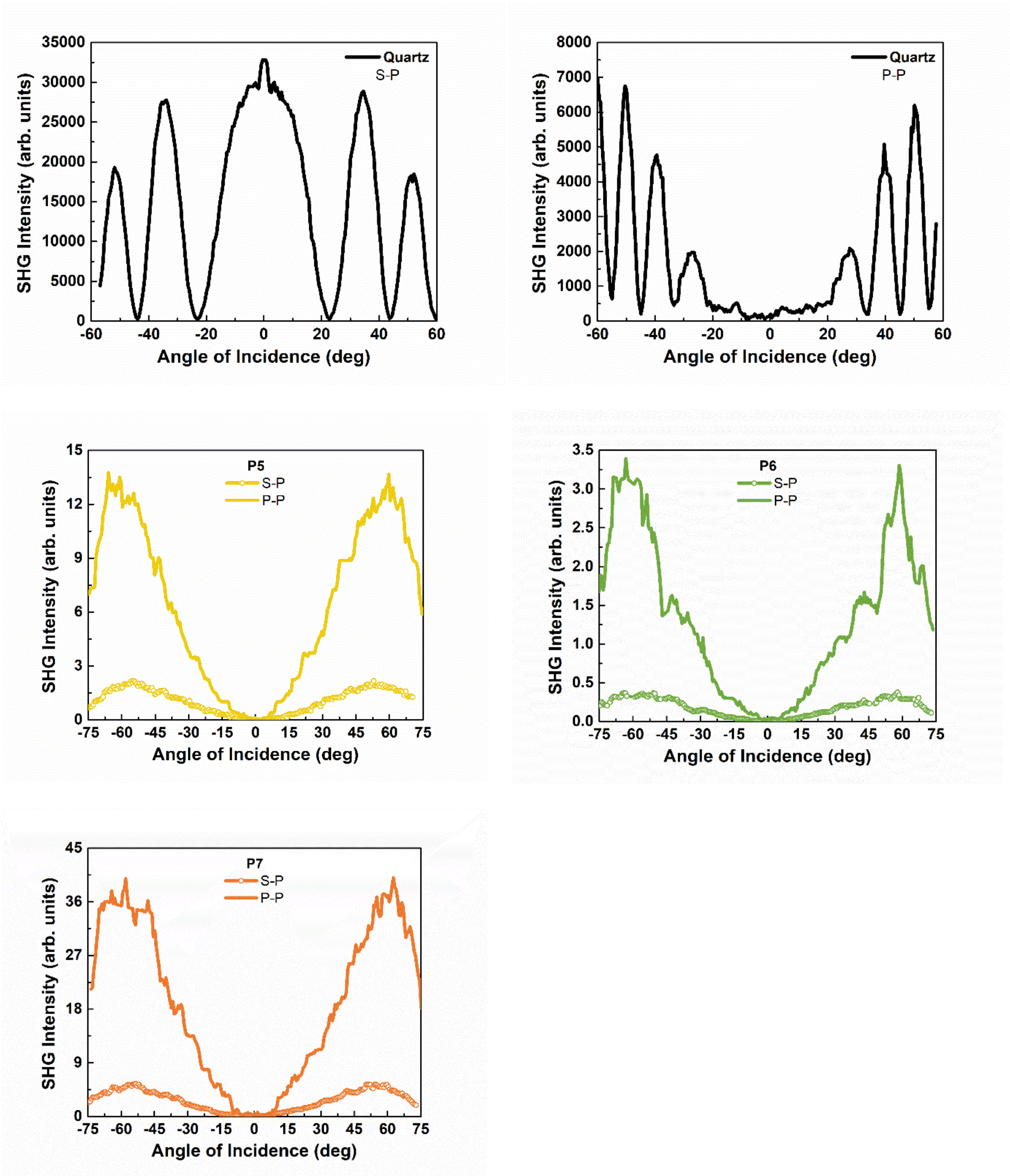

Figure S11: SHG intensities as a function of incident angle of investigated thin films in S-P and P-P polarized laser irradiation.

Fig. S11 displays SHG intensities as a function of incident angle of the studied pyrazoline thin films. Notably, SHG process is strongly dependent on the laser polarization. We observed that investigated samples favour P-P polarization, which is associated with an enhanced response in this configuration.

$\chi^{(2)}$ values of **P2-7** thin films :

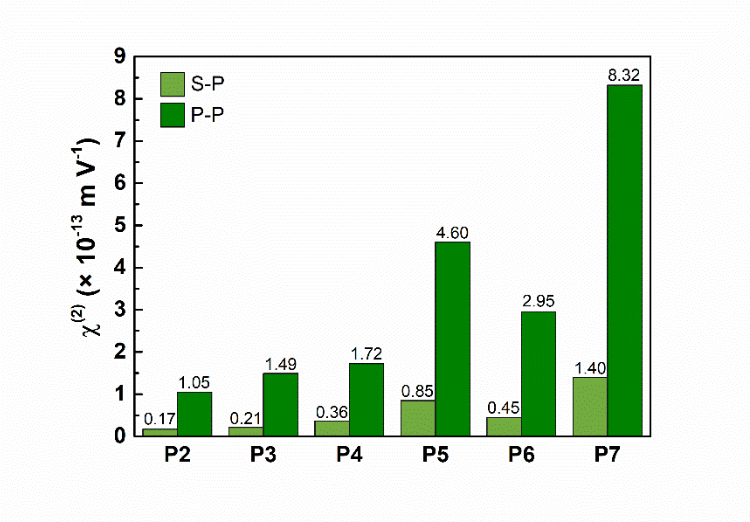

Figure S12: Histogram displaying second-order NLO susceptibilities of **P2-7** thin films.

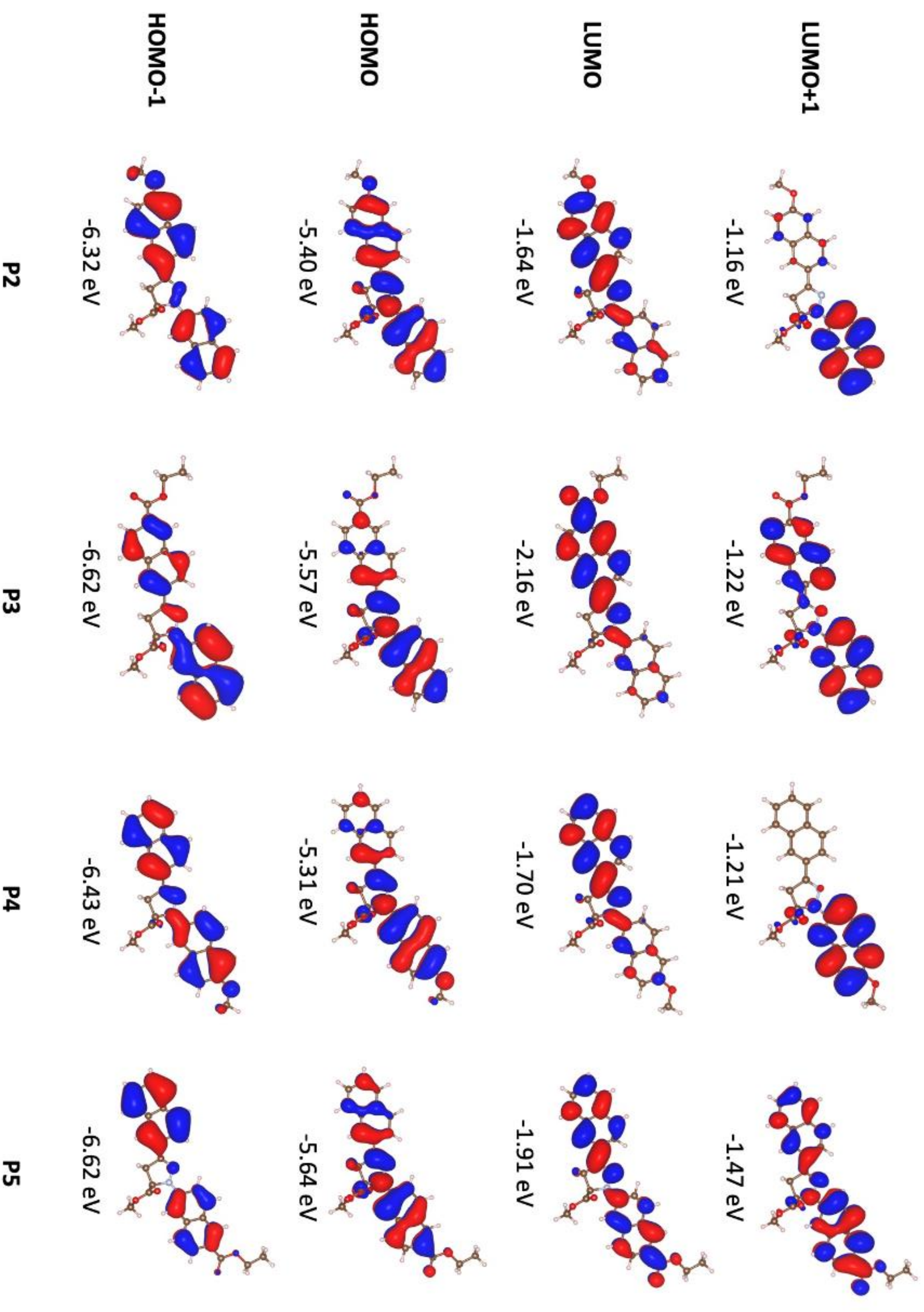

Figure S13: Contour plots (isosurface value = 0.02 au) and energy levels of the frontier molecular orbitals levels of pyrazolines **P2**-**P5** at the PBE0/6-311+G(d,p) level with a PCM model of THF.

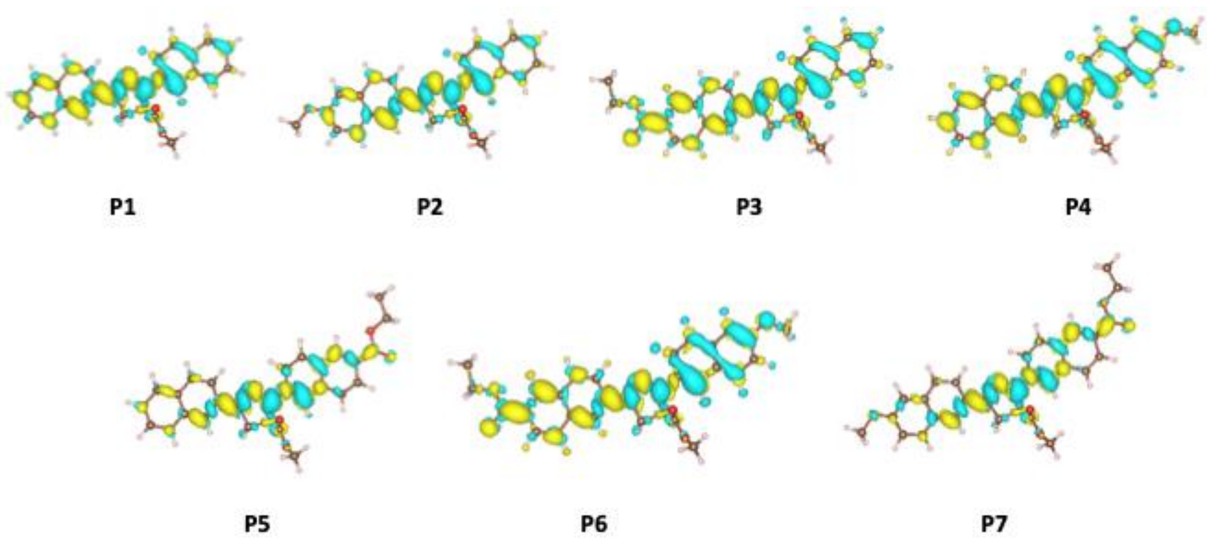

Figure S14: Contour plots (iso-surface value = 0.001 au) of the electronic density difference between the ground and first excited state for the excitation (absorption) of **P1**-**P7** at the PBE0/6-311+G(d,p) level with a PCM model of THF.

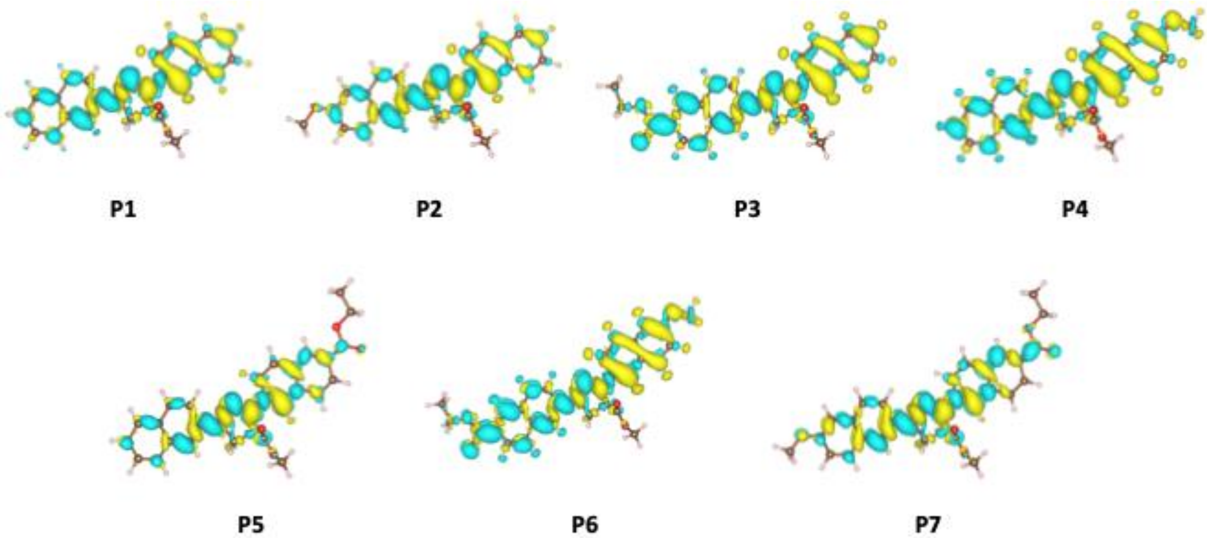

Figure S15: Contour plots (iso-surface value = 0.001 au) of the electronic density difference between the ground and first excited state for the de-excitation (emission) of **P1**-**P7** at the PBE0/6-311+G(d,p) level with a PCM model of THF.

Table S1: Computed photophysical properties for **P1**, **P6** and **P7** at the PBE0/6-311+G(d,p) level in gas phase.

Cpd	λ_{abs} [nm] (f)	*Transition description*	λ_{em} [nm] (f)	Stokes shift [cm^{-1}]
P1	379 (0.99)	HOMO-LUMO	466 (0.72)	4926
P6	430 (0.97)	HOMO-LUMO	544 (0.71)	4873
P7	384 (1.50)	HOMO-LUMO	438 (1.29)	3210

Table S2: Computed photophysical properties for **P1**, **P6** and **P7** at the CAM-B3LYP/6-311+G(d,p) level with a PCM model of THF.

Cpd	λ_{abs} [nm] (f)	Transition description	λ_{em} [nm] (f)	Stokes shift [cm^{-1}]
P1	348 (1.45)	HOMO-LUMO	428 (1.65)	5371
P6	375 (1.57)	HOMO-LUMO	460 (1.80)	4927
P7	356 (1.95)	HOMO-LUMO	428 (2.17)	4725

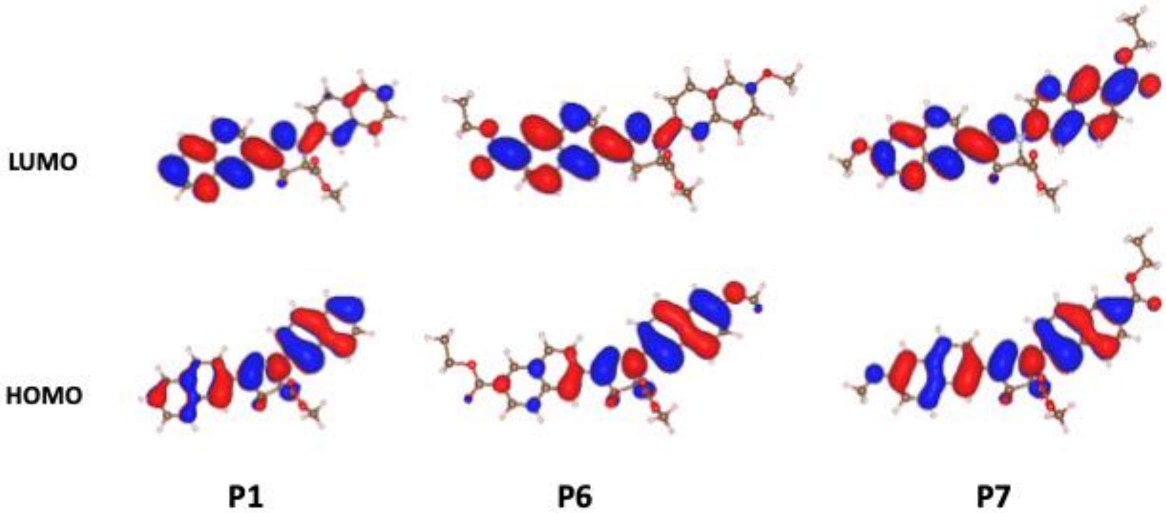

Figure S16: Contour plots (isosurface value = 0.02 au) of the frontier molecular orbitals levels of pyrazolines **P1**/**P6/P7** at the CAM-B3LYP/6-311+G(d,p) level with a PCM model of THF.

Table S3: Computed charge transfer characteristics between the ground and the first excited state for **P1**-**P7** at the PBE0 /6-311+G(d,p) level with a PCM model of THF, for the absorption and the emission process. Charges transferred Q_{CT} are given in atomic units and transfer distances D_{CT} *are* in Angströms.

Cpd	**Q_{CT} abs**	**D_{CT} abs**	**Q_{CT} em**	**D_{CT} em**
P1	0.65	4.14	0.61	4.22
P2	0.59	3.58	0.55	3.57
P3	0.75	5.24	0.71	5.35
P4	0.71	4.86	0.71	5.03
P5	0.55	1.60	0.50	2.31
P6	0.81	5.82	0.80	6.03
P7	0.52	0.67	0.46	0.49